

## A 4<sup>th</sup>-order accurate finite volume method for ideal and resistive classical and special relativistic MHD in the PLUTO code

---

V. Berta,<sup>a,\*</sup> A. Mignone,<sup>a</sup> M. Bugli<sup>a,b</sup> and G. Mattia<sup>c</sup>

<sup>a</sup>*Dipartimento di Fisica, Università di Torino,  
via P. Giuria 1, 10125 Torino, Italy*

<sup>b</sup>*Université Paris-Saclay, Université Paris Cité, CEA, CNRS, AIM,  
91191, Gif-sur-Yvette, France*

<sup>c</sup>*INFN, Sezione di Firenze,  
Via G. Sansone 1, I-50019 Sesto Fiorentino, Italy  
E-mail: [vittoria.bera@unito.it](mailto:vittoria.bera@unito.it), [andrea.mignone@unito.it](mailto:andrea.mignone@unito.it),  
[matteo.bugli@unito.it](mailto:matteo.bugli@unito.it), [mattia@fi.infn.it](mailto:mattia@fi.infn.it)*

We present a novel implementation of a genuinely 4<sup>th</sup>-order accurate finite volume scheme for multidimensional classical and special relativistic magnetohydrodynamics (MHD) in both ideal [1] and resistive [2] regimes based on the constrained transport (CT) formalism in the PLUTO code [3, 4]. Our scheme is rooted over the method originally proposed by McCorquodale and Colella [5] but introduces several novel aspects when compared to its predecessors, yielding a more efficient computational tool. Among the most relevant ones, our scheme exploits pointwise to pointwise reconstructions (rather than one-dimensional finite volume ones). It employs all the generalized upwind averaging techniques of the upwind constrained-transport (UCT) method of Mignone and Del Zanna [6] to evaluate the electromotive force (EMF) at zone edges, with the addition of a new relativistic UCT-GFORCE average, and ensures robustness through sophisticated limiting strategies that include both a discontinuity detector and an order reduction procedure. We thoroughly tested such method, producing results that confirm its efficiency compared to traditional low order schemes.

*High Energy Phenomena in Relativistic Outflows VIII (HEPROVIII)  
23-26 October, 2023  
Paris, France*

---

\*Speaker

## 1. Introduction

The modeling of astrophysical plasmas is nowadays demanding for more efficient and accurate numerical schemes for solving the equations of ideal and resistive, classical and special relativistic magnetohydrodynamics (MHD, RMHD, Res-RMHD). Physical interest is increasingly directed towards the investigation of highly nonlinear flows featuring both smooth and discontinuous solutions, with a great deal of attention being devoted to enhance the accuracy of the underlying numerical methods while retaining stability and computational efficiency. Concurrently, the investigation of relativistic plasma dynamics holds crucial importance in understanding the complex nature of high-energy astrophysical phenomena. Under typical astrophysical conditions, the ideal framework well describes processes occurring on rapid time scales. Nevertheless, the evolving flow dynamics can cause the formation of local regions with steep gradients, such as current sheets, where the influence of resistivity can no longer be ignored. It appears then clear the necessity of numerical simulations of astrophysical plasmas beyond the ideal magnetohydrodynamics (MHD) assumptions that take into account the contribution of finite plasma conductivity.

In the last decade several efforts have been made to design higher than 2<sup>nd</sup>-order numerical methods both for Finite Difference (FD), and Finite Volume (FV) approaches. 4<sup>th</sup>-order schemes, in fact, can reach unprecedented performances overstepping the limits of traditional 2<sup>nd</sup>-order frameworks because of their intrinsic lower dissipation properties. In a resistive framework, a decrease in numerical dissipation means that we can probe the dynamical impact of more realistic (i.e. lower) values of physical magnetic dissipation, which needs to dominate over the numerical one in any reliable Res-RMHD model [7]. In addition, smooth solutions are improved at much faster rates, yielding enhanced convergence and henceforth a computational efficiency that increases with the dimensionality of the problem and with resolution.

## 2. The 4<sup>th</sup>-order method

Our 4<sup>th</sup>-order accurate numerical scheme targets any time-dependent hyperbolic system of equations of the form

$$\frac{\partial U}{\partial t} + \nabla \cdot F = S(U), \quad (1)$$

with  $U$  state vector of conservative quantities,  $F$  flux tensor, and  $S(U)$  the source terms (if present). In the FV fashion, a semi-discrete method of lines approximates Eq. 1, yielding

$$\frac{d \langle U \rangle_c}{dt} = - \left( \frac{\hat{F}_{x,x_f} - \hat{F}_{x,x_f-\hat{e}_x}}{\Delta x} + \frac{\hat{F}_{y,y_f} - \hat{F}_{y,y_f-\hat{e}_y}}{\Delta y} + \frac{\hat{F}_{z,z_f} - \hat{F}_{z,z_f-\hat{e}_z}}{\Delta z} \right) + \langle S \rangle_c. \quad (2)$$

where  $\langle U \rangle_c$  is the cell volume average of the conservative quantity  $U$  (e.g.,  $U = \{\rho, \rho \mathbf{v}, \mathcal{E}, \mathbf{B}\}$ ),  $\hat{F}_{x,x_f}$  is the surface average of the  $x$ -component of the flux over a face perpendicular to the  $x$ -direction,  $\hat{F}_{x,x_f-\hat{e}_x}$  is the surface average of the same component over the opposite side of the cell, (similarly for the other flux terms along the  $y$ - and  $z$ -directions), and  $\langle S \rangle_c$  is the cell volume average of the source terms. At 2<sup>nd</sup>-order accuracy, point values can be interchanged with volume or surface averages before the mapping to primitive values. This property, however, does no longer hold for higher order schemes, where one has to distinguish the cell-centered point value from its volume

average and, likewise, the face-centered flux from its surface average. In our scheme we take into account this aspect by means of the conversion relations

$$Q_c = \langle Q \rangle_c - \frac{\Delta \langle Q \rangle_c}{24}, \quad \langle Q \rangle_c = Q_c + \frac{\Delta Q_c}{24} \quad (3)$$

originally introduced by McCorquodale & Colella [5], using the Laplacian operator  $\Delta Q_c \equiv \Delta^x Q_c + \Delta^y Q_c + \Delta^z Q_c$ , with components given by  $\Delta^i Q_c \equiv (Q_{c-\hat{e}_i} - 2Q_c + Q_{c+\hat{e}_i})$ , and  $i = x, y, z$ . In Eq.(3),  $\langle Q \rangle_c$  represents any component of  $\langle U \rangle_c$ , and likewise for its pointwise counterpart  $Q_c$ . From the first relation in Eq.(3) we can retrieve the ensemble of primitive variables  $V_c$  (e.g.,  $V = \{\rho, \mathbf{v}, p, \mathbf{B}\}$ ). Spatial reconstruction at cell interfaces is then performed, for the first time in the literature of FV schemes, by a version of the MP5 [8] and the WENOZ [9] algorithms based on pointwise values that lower the algorithmic complexity of the overall scheme by retaining the 4<sup>th</sup>-order accuracy with fewer operations per step and without even enlarging the stencil size [1]. Moreover, this new feature is reducing the number of Riemann problems to be solved per direction, leading to a more efficient and cost-effective scheme. Occasionally, Eq. 3 may introduce negative values in density and energy resulting in the growth of numerical instabilities. Robustness is ensured with a local discontinuity detector to distinguish smooth solutions from discontinuous ones when determining the function local point value from its cell average. The upwind fluxes obtained by solving the Riemann problem are then surface-averaged by means of the transverse Laplacian operators  $\Delta_\perp^x$

$$\hat{F}_{x,x_f} = F_{x_f} + \frac{\Delta_\perp^x F_{x_f}}{24}. \quad (4)$$

Regarding temporal integration, we employ a semi-discrete approach based on a five-stage 4<sup>th</sup>-order explicit strong stability preserving Runge-Kutta method (eSSPRK(5,4), [10]) for ideal frameworks, and an implicit-explicit (IMEX) strong stability preserving (SSP) Runge Kutta (RK) scheme of the third order (IMEX(4,3,3), [11]) for the Res-RMHD one, coping with the stiff relaxation term in Ampere's law, which poses very strict constraints on the time step.

The solenoidal condition of the magnetic field is fulfilled by means of a high-order formulation of the generalized upwind constrained transport (UCT, [6]) algorithm, which ensures a divergence-free magnetic field up to machine accuracy, and works well with any generic upwind average. Source terms are added analogously after suitable averaging via the Laplacian operators.

### 3. Numerical tests

#### 3.1 The 3D circularly polarized ideal Alfvén waves

We assessed the convergence of the method by considering the oblique propagation of circularly polarized Alfvén waves, which are exact non-linear solutions of the (R)MHD equations. This test revealed that the measured convergence rates match the expected order of accuracy as shown in the left panel of Fig. 1. One of the advantages of adopting 4<sup>th</sup>- (or higher) order schemes is that, for problems without sharp gradients, the increase of accuracy brought by the scheme leads to a saving in computational time for fixed accuracy. Let  $\epsilon_p = CN^{-p}$  ( $p = 2, 4$ ) be the final numerical error, with  $p$  order of the scheme and  $C$  an unknown constant of  $\propto O(1)$ . For a fixed accuracy  $\epsilon_p$  it is possible to demonstrate, after some straightforward algebra, that 2<sup>nd</sup>- and 4<sup>th</sup>-order schemes will

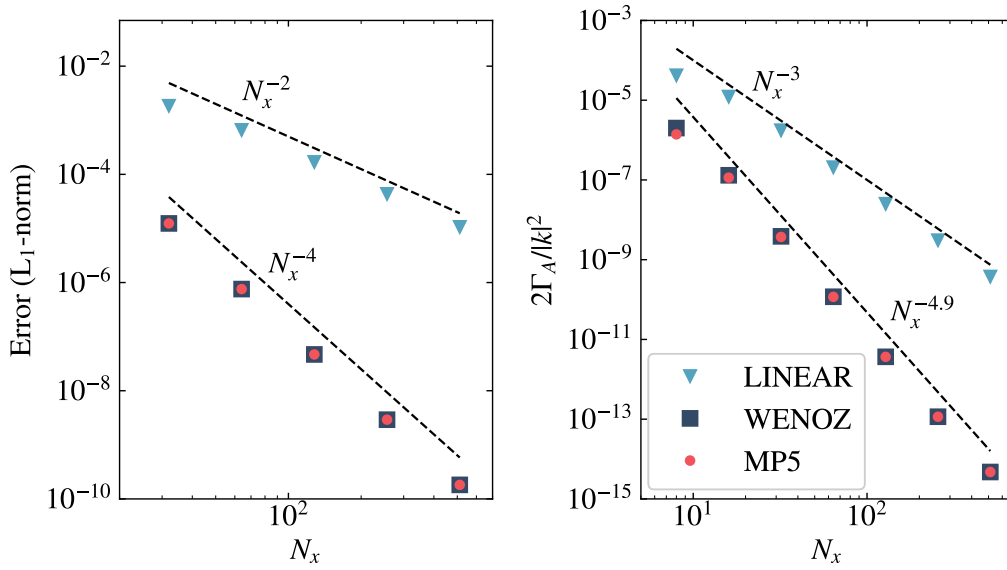


**Figure 1:**  $L_1$ -norm errors (left panel) and numerical diffusion (right panel) for the 3D circularly polarized Alfvén wave test in the MHD regime (solid lines) and RMHD (dashed-dotted lines) as functions of the grid resolution  $N_x$  with 2<sup>nd</sup>- and 4<sup>th</sup>-order numerical schemes. The dashed lines give the ideal convergence slope (left panel) and a reference slope for the numerical diffusion (right panel).

achieve  $\epsilon_2 \sim \epsilon_4$  with  $N_4 \sim \sqrt{N_2}$  grid points. As shown in Fig. 1, the fixed accuracy of  $10^{-4}$  is reached at  $N_2^3 = 512^3$  for the 2<sup>nd</sup>-order, and at  $N_4^3 = 34^3$  for the 4<sup>th</sup>-order, resulting in a reduction of the computational time by a factor  $\sim 10^4$ . Another advantage of using a more accurate scheme is the reduction of the numerical dissipation due to the round-off errors introduced by the grid discretization. By measuring the diffusion intrinsic to the numerical scheme that inevitably damps the Alfvén waves ([12] we estimated an overall decay rate of  $\sim N^{-4.9}$  for the 4<sup>th</sup>-order scheme versus only  $\sim N^{-3.0}$  for the 2<sup>nd</sup>-order (right panel of Fig. 1).

### 3.2 The relativistic current sheet

In our scheme we use a high-order formulation of the Upwind Constrained Transport method employing all the EMF averages of [6] with the additional introduction of a new UCT-GFORCE average in the RMHD framework to ensure  $\nabla \cdot \mathbf{B} = 0$ . Pointwise reconstructions reduce the number of transverse ghost zones to reconstruct the electric field at edges, resulting in a more efficient UCT algorithm. The ideal relativistic current sheet shown in Fig. 2 reproduces the one by [13], but with a more accurate and less dissipative solver (GFORCE rather than a linear solver).

### 3.3 The 3D MHD blast wave

The novel scheme ensures robustness by means of a sophisticated limiting strategy as demonstrated by the severe blast configuration shown in Fig. 3 initially presented by Balsara & Spicer [14], where  $B_0 = 100/\sqrt{4\pi}$ ,  $p_{\text{out}} = 1$ , and  $p_{\text{in}} = 10^3$ . The limiter acts in two stages of the algorithm:

1. during the conversion  $\langle U_c \rangle \Rightarrow U_c$  for a "reverting to 2<sup>nd</sup>-order" procedure based on either a Jameson's shock sensor [15] or by a more sensitive indicator that takes into account higher

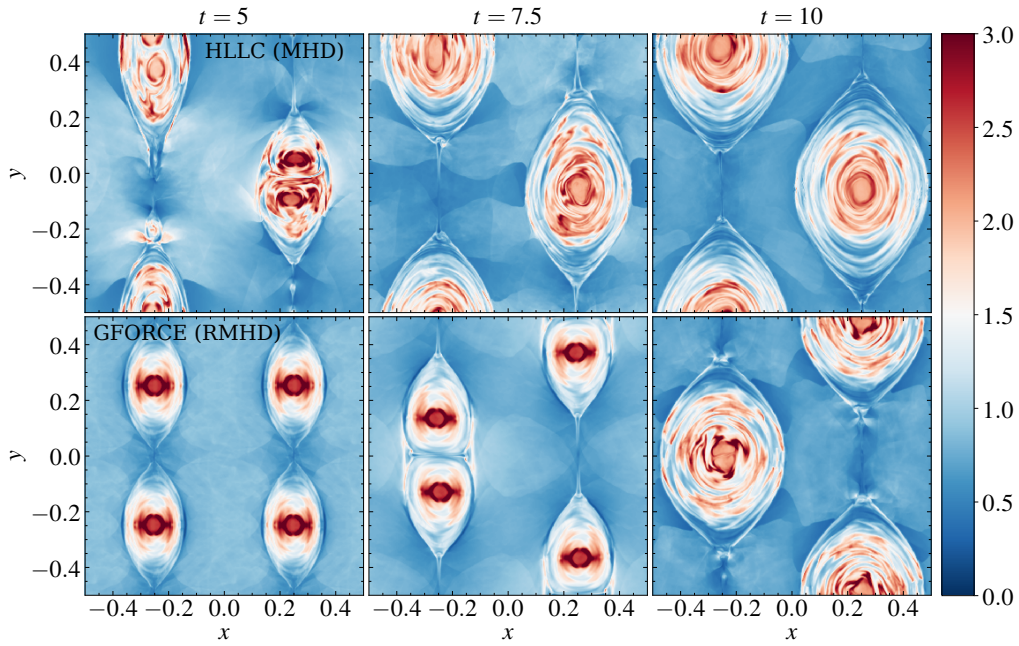


**Figure 2:** Coloured maps for the density snapshots of the classical (top panel) and relativistic (bottom panel) current sheet.

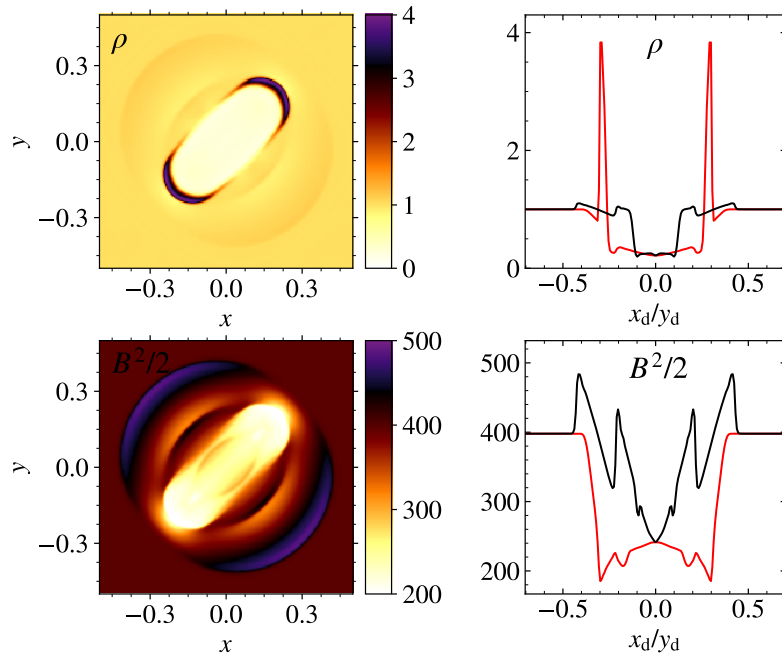


**Figure 3:** MHD 3D blast wave problem at  $t = 0.1$ . The left panels show density (top, in logarithmic scale), and magnetic energy (bottom) at  $z = 0$ . The right panels instead show the density (top) and magnetic energy density (bottom) on the major (red line) and minor (black line) diagonals.

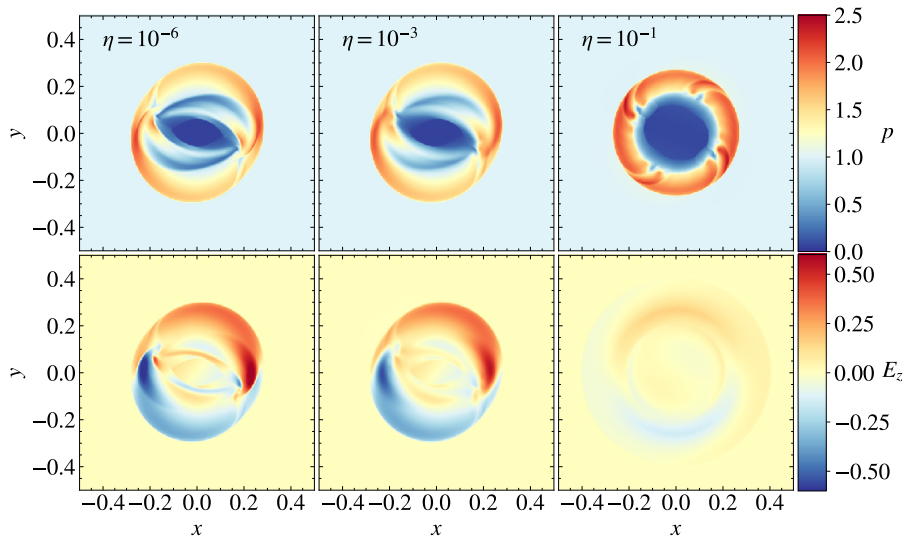


**Figure 4:** Snapshots of the gas pressure  $p$  (upper panels), and profiles of  $E_z$  (lower panels) for the resistive rotor test at its final time  $t = 0.3$ . Each column reproduces the test performed with different resistivities  $\eta$ , from the nearly ideal case  $\eta = 10^{-6}$  (left-hand panels), the intermediate case  $\eta = 10^{-3}$  (central panels), and the resistive case  $\eta = 10^{-1}$  (right-hand panels).

order derivatives' ratio [16];

2. during reconstruction at interfaces by means of an order reduction procedure that selects a linear reconstruction when oscillations are generated.

This test has so far been feasible only with 2<sup>nd</sup>-order schemes.

### 3.4 The Res-RMHD rotor

This test consists of a high density disk rotating at relativistic speed with an angular velocity of  $\omega = 8.5$  code units in a uniform ambient medium. As shown in Fig. 4, we performed a set of simulations with increasing resistivities  $\eta = 10^{-6}, 10^{-3}, 10^{-1}$  to explore the capabilities of the scheme in dealing with progressively stiffer terms and assess that the complex pattern of shocks and torsional Alfvén waves is correctly reproduced.

## 4. Conclusions

With the present work we presented a genuinely 4<sup>th</sup>-order accurate finite volume scheme for both ideal and resistive (R)MHD accounting several innovative aspects that yield an accurate, robust and efficient computational tool. Among the most relevant innovations there is the introduction of pointwise to pointwise reconstruction operations that ease up the structure of the scheme, the generalization of the UCT-GFORCE average to relativistic MHD, and the introduction of a limiter that allows the 4<sup>th</sup>-order scheme to carry out severe tests. Future developments will include the extension of the scheme to non-Cartesian geometries such as cylindrical and spherical reference frames, and in General-Relativistic frameworks.

## References

- [1] V. Berta, A. Mignone, M. Bugli and G. Mattia, *A 4<sup>th</sup>-order accurate finite volume method for ideal classical and special relativistic mhd based on pointwise reconstructions*, *JCP* **499** (2024) 112701.
- [2] A. Mignone, V. Berta, M. Rossazza, M. Bugli, G. Mattia, L.D. Zanna et al., *A fourth-order finite volume scheme for resistive relativistic magnetohydrodynamics*, *MNRAS* (2024) .
- [3] A. Mignone, G. Bodo, S. Massaglia, T. Matsakos, O. Tesileanu, C. Zanni et al., *Pluto: A numerical code for computational astrophysics*, *ApJS* **170** (2007) 228.
- [4] A. Mignone, C. Zanni, P. Tzeferacos, B. van Straalen, P. Colella and G. Bodo, *The pluto code for adaptive mesh computations in astrophysical fluid dynamics*, *ApJS* **198** (2012) 7.
- [5] P. McCorquodale and P. Colella, *A high-order finite-volume method for conservation laws on locally refined grids.*, *Commun. Appl. Math. Comput. Sci.* **6** (2011) 1.
- [6] A. Mignone and L.D. Zanna, *Systematic construction of upwind constrained transport schemes for MHD*, *JCP* **424** (2021) 109748.
- [7] G. Mattia, L. Del Zanna, M. Bugli, A. Pavan, R. Ciolfi, G. Bodo et al., *Resistive relativistic MHD simulations of astrophysical jets*, *A&A* **679** (2023) A49.
- [8] A. Suresh and H.T. Huynh, *Accurate Monotonicity-Preserving Schemes with Runge Kutta Time Stepping*, *JCP* **136** (1997) 83.
- [9] R. Borges, M. Carmona, B. Costa and W.S. Don, *An improved weighted essentially non-oscillatory scheme for hyperbolic conservation laws*, *JCP* **227** (2008) 3191.
- [10] R.J. Spiteri and S.J. Ruuth, *A new class of optimal high-order strong-stability-preserving time discretization methods*, *SIAM Journal on Numerical Analysis* **40** (2002) 469.
- [11] L. Pareschi and G. Russo, *Implicit-explicit runge-kutta schemes and applications to hyperbolic systems with relaxation*, *Journal of Scientific Computing* **25** (2005) 129.
- [12] A. Mignone, *A simple and accurate Riemann solver for isothermal MHD*, *Journal of Computational Physics* **225** (2007) 1427.
- [13] J.N. de la Rosa and C.-D. Munz, *xtroem-fv: a new code for computational astrophysics based on very high order finite-volume methods – II. Relativistic hydro- and magnetohydrodynamics*, *Monthly Notices of the Royal Astronomical Society* **460** (2016) 535.
- [14] D.S. Balsara and D.S. Spicer, *A Staggered Mesh Algorithm Using High Order Godunov Fluxes to Ensure Solenoidal Magnetic Fields in Magnetohydrodynamic Simulations*, *JCP* **149** (1999) 270.
- [15] A. Jameson, W. Schmidt and E. Turkel, *Numerical solution of the Euler equations by finite volume methods using Runge Kutta time stepping schemes*, in *AIAA, 14th Fluid and Plasma Dynamics Conference*, vol. 15, 1981.

- [16] M.L.B. de Oliveira and V.A. Pires, *Analysis of a high-order finite difference detector for discontinuities*, *Int. J. Comput. Math.* **94** (2017) 676.